

LabView Program for Thermal Conduction Measurements

Erica Douglas

College of Liberal Arts and Sciences, University of Florida

Introduction

Some antiferromagnetic geometric shapes have unique and complex behaviors. In the case of a triangular lattice, once two of the three spins on the lattice are anti-aligned in order to appease the antiferromagnetic (AF) behavior of the material, the third spin is unable to point in a direction which will be opposite to the other two spins while minimizing the energy states. Hence, the symmetry of the triangular lattice is not compatible with AF interactions. This situation is known as triangular geometric frustration.¹ The consequence of the geometric frustration on the cooperative behavior can affect the ground state selection which is established by interactions such as the “next-nearest-neighbor.”² Geometric frustration can also affect quantum fluctuations and usually results in various degenerate ground states.^{1,2}

Geometrically frustrated antiferromagnets are studied in order to determine what happens when the triangular lattice prevents the spin configuration from becoming simple and ordered. There are very few materials, however, which exhibit this behavior.⁴ Cs_2CuBr_4 is an example of a crystal which displays the triangular lattice, AF interactions, and it has a spin $S = 1/2$. Magnetocaloric-effect and specific-heat measurements were performed on a sample of Cs_2CuBr_4 in order to determine the phases, such as up-up-down (uud) of the spins. The focus of the research was on that of the specific-heat measurements. Specific-heat data uncovers the “dramatic enhancement of the magnon gap.”³ This, in turn, gives way to the presence of the Dzyaloshinskii-Moriya interaction, though only weak.

There are several factors that can affect specific-heat measurements. One of these is a fluctuation in the thermal conductance of the weak links in the calorimeter used for taking specific-heat measurements. In order to verify that the thermal conductance is consistent over time and magnetic fields, an addition to the LabView program used to acquire data was written.

Background

In order to understand essential features of geometrically frustrated magnetism, one can look at an isotropic Heisenberg model consisting of classical spins interacting via the nearest neighbor exchange described by the Hamiltonian for a layered triangular lattice:

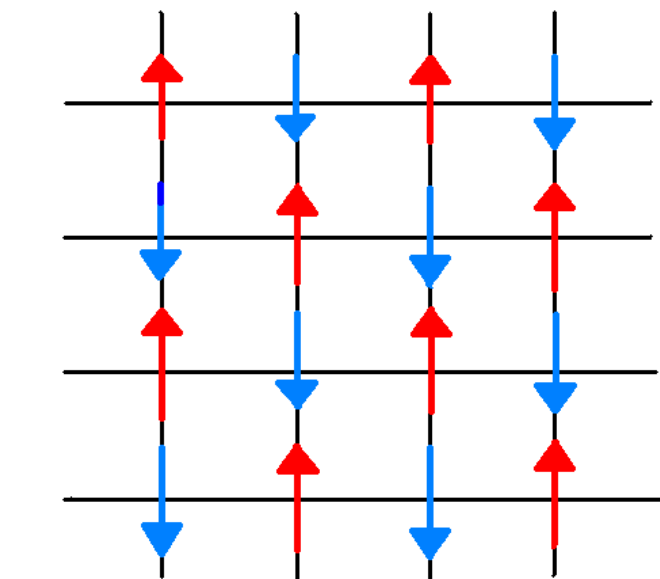
$$H = - \sum_{i < j} J_{ij} S_i \cdot S_j \quad (1)$$

where S is a unit length, classical three-component vector and J_{ij} is the strength of the exchange interaction between spins at sites i and j . This can be simplified by looking at a simple set of Hamiltonians that describe only antiferromagnetic interactions of nearest neighbors:

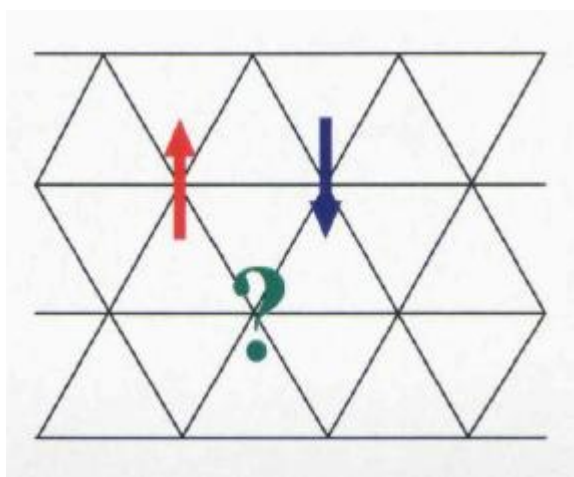
$$H = J \sum_{i,j} S_i S_j \quad (2)$$

J , with a positive exchange energy, will favor antiparallel alignment of the spins S . This is labeled by the site indices of i and j . The sum is then taken over the nearest-neighbor bonds and the Heisenberg vector spins S are again a three component vector where $S = (S_x, S_y, S_z)$ of spin length $|S|$ which is again fixed. Each spin has two degrees of freedom. Since the length of the spin is fixed, it is “free to take any value on the surface of a sphere.”¹ These two degrees of freedom can be thought of as longitude and latitude for this case. The total number of degrees of freedom in the ground state (F) can be estimated to be $D - K = F$, where D is the total number of degrees of freedom of the spins and K is the total number of constraints that have to be met in order for the system to be in a ground state. This, however, may not always be the case since the constraints due to the equations may not be independent or they are mutually exclusive. Typically, when the total spin sums to zero, the state is in its ground state. When the magnetization plateau is present in Cs_2CuBr_4 , it signifies that the material is in the ground state. This ground state can be present as a “spin liquid, a collection of spin multimers, or an ordered state that is collinear with the magnetic field.”³

With respect to Equation 1, $J_{ij} < 0$, when the spins of the system are interacting antiferromagnetically in a triangular lattice. In the case of magnetic Cu^{2+} , ions are located on the CuBr_4^{2-} tetrahedra and form the triangular lattice in the bc plane. In the b direction, the Cu^{2+} nearest-neighbor exchange, J_1 , is larger than J_2 in the other “principal directions” in the bc plane.³ According to Tsujii et al., the ratio of $J_2/J_1 = 0.74$ for Cs_2CuBr_4 .³ Maximum geometric frustration occurs at $J_2/J_1 = 1$, which indicates that Cs_2CuBr_4 is very close to this maximum frustration. In comparison to Cs_2CuCl_4 , another triangular frustrated antiferromagnet with $S = 1/2$, the ratio of J_2/J_1 ranged from 0.34 to 0.37.³



(a)



(b)

Figure 1: a) Illustration of antiferromagnetic spins on a lattice b) Triangular geometrically frustrated antiferromagnet¹

In zero-field, the Heisenberg model of the nearest-neighbor in zero-field exhibits 120° spin order.³ An extremely important finding in the crystal is that of a magnetization plateau. It is in this region that the magnetization of the material is constant despite the fact that magnetic field is increasing around it.⁵ In order for the magnetization plateau to exist, the spin system must satisfy the plateau condition of $n(S - m) = \text{integer}$, where n is the period of the spin state, S is the magnitude of the spin, and m is magnetization per site in the unit of $g\mu_B$.⁵ Essentially, this effect arises from the gap in energy of the

“low-lying magnetic excitations” and is a result of the continuous rotational symmetry of the Hamiltonian.³

In order to determine the heat capacity of a sample, heat is applied to the sample in the form of

$$C = \Delta Q / \Delta T, \tag{3}$$

where C is the specific-heat, ΔQ is the change in heat applied to the sample, and ΔT is the change in temperature of the sample. Thermal relaxation is used in order to determine the specific-heat. Once the system is in a steady state with current flowing through the system, as shown in Fig. 2, the power is then turned off. This, in turn, leads to a decay in temperature (voltage) to $T_0(0)$ within a time constant of

$$C = k(RC),$$

where k is the thermal conductance. When the thermal conductance of a sample is low, the specific-heat of it may not be accurately measured with this method. This is due to a temperature gradient that becomes present in the sample.⁶ The internal relaxation time, denoted by τ_2 , accounts for this effect by

$$\tau_2 = C/k_{int},$$

where k_{int} is the thermal conductance of the sample.⁶

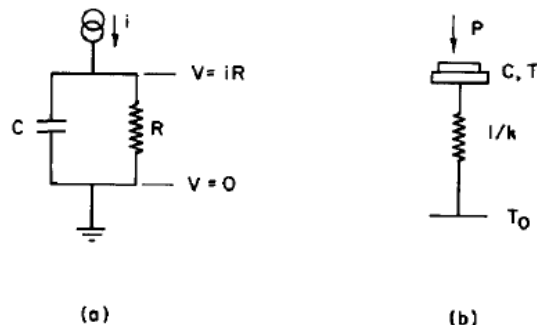


Figure 2: a) Electrical schematic of thermal relaxation method b) Heat flow schematic⁶

Apparatus

A relaxation calorimeter was used to gather both specific heat and magneto-caloric effect data. A dilution refrigerator was used in order to cool the calorimeter and the sample. Compared to the typical quasi-adiabatic calorimeters, this method allows the experimenters to be in the milli-Kelvin range. Fig. 3 is a schematic of the calorimeter.

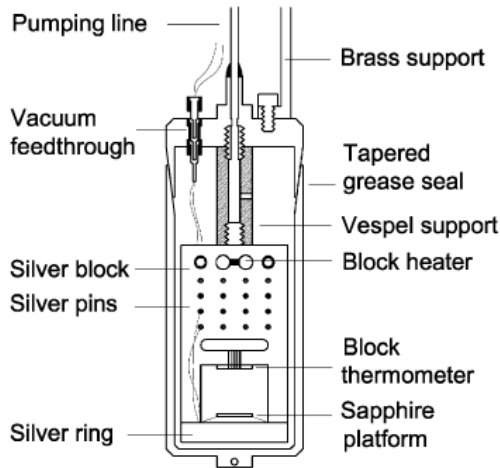


Figure 3: Schematic of the calorimeter (cross section)

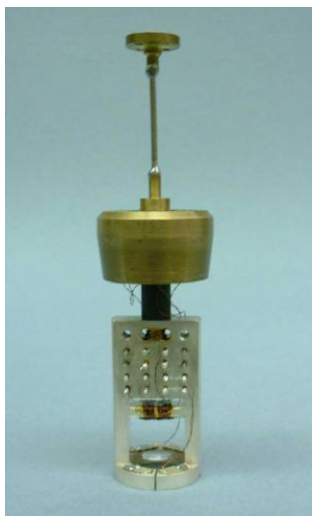


Figure 4: Calorimeter used for a top-loading dilution refrigerator

The silver block, as shown in Fig. 3, is used as a thermal reservoir. This is made entirely of silver in order to prevent the time constant from becoming too long. Silver was used because of its very small nuclear heat capacity. In order to monitor the temperature of the silver block, a 220 Ω Speer carbon resistor that was ground to a thickness of 0.5 mm. Another important feature of the calorimeter is the brass casing that encloses it. The brass prevents thermal radiation and heating due to eddy-currents. It also thermally isolates the liquid helium in the mixing chamber from the calorimeter.⁷ The sample is placed on a platform made of sapphire. This design of the calorimeter allows the experimenters to use samples that are small, on the order of a few milligrams. This is essential since it is often difficult to obtain bulk crystals. The platform heater is constructed from a thin evaporated layer of a 7% Ti-Cr alloy.⁷ The platform is actually supported by the electrical leads for the thermometer and the heater. These leads also provide a weak thermal link between the platform and the silver ring.

In order to calculate the heat capacity of a sample that is placed on the sapphire platform, the temperature difference

is measured, ΔT , between the silver ring and the weak thermal link of the platform. Once the Ti-Cr heater is turned off, the relaxation time is measured by the use of a lock-in amplifier as well as the null detector of a Wheatstone bridge.⁷ In order to actually obtain the heat capacity of the sample, the thermal conductance of the weak links are measured and a non-linear least-squares fit is performed on the relaxation data.

Method

Once measurements at varying magnetic fields are taken and the calorimeter is calibrated, the specific-heat measurements should be consistent. However, it is quite possible that the thermal conductance of the weak links between the silver thermal reservoir and the sapphire platform where the sample is placed fluctuates over time. This may be due to a buildup of material on the weak links. As a change in the thermal conductance can ultimately effect where the phase transitions appear, it is extremely important to make sure that the calorimeter is calibrated at all times. The addition, the LabView program was designed in such a way that a separate file is written and appended for the platform voltage, independent of the master file. Previously, voltages were read directly from the voltmeter and manually written down. These values were then recorded into a computer file, a process open to user error. Thus, this program is intended to reduce user error and allow analysis on the thermal conductance to be carried out independent of the master file.

As can be seen in Fig. 5, a For loop was designed with five iterations. Within this For loop, the Keithley sub-VI is used to read the voltage of the platform. This sub-VI reads in the platform heater GPIB address, the platform heater current in micro-amps as a local read variable, and the platform heat current GPIB address. This in turn allows the sub-VI to determine the resistance in ohms as well as the voltage of the platform. The voltage is read five times and averaged in order to obtain more accurate data.

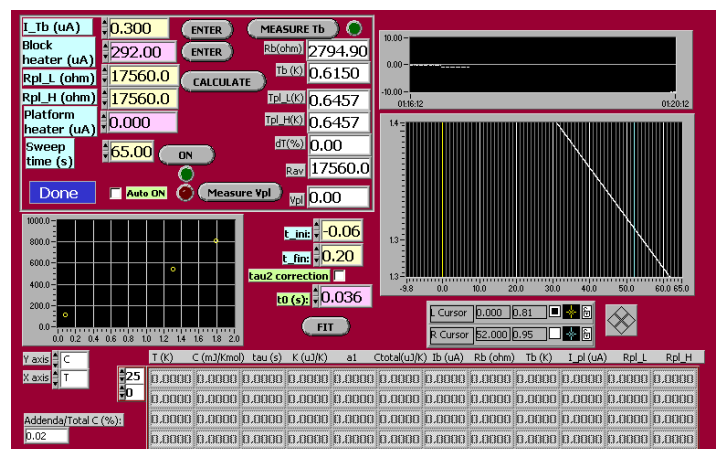


Figure 5: Front panel of specific-heat LabView program

Block T calib. file: bt051803.dat
 Platform coeff. file: pt091803.dat
 Conduct. coeff. file: ck051803lo.dat
 Data file directory: c:\users\tsuji\cp\
 Cp data file: bamo_mc.dat
 Vpl data file: []

GPIB addresses:
 Block heater I: 12
 Platform heater I: 17
 Platform Heater V: []
 Block therm. I: 24
 Block therm. V: 26

Figure 6: User required inputs for GPIB addresses and data file names

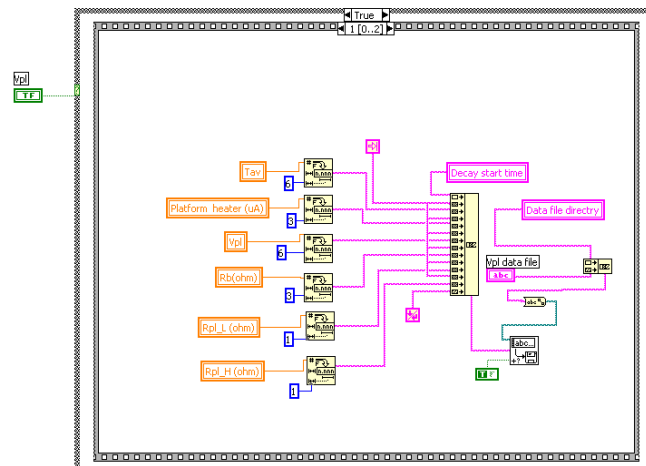


Figure 8: Second sequence of true case

Conclusion

In summary, triangular geometrically frustrated anti-ferromagnets can provide insightful evidence into the phases as well as enhancing the magnon gap. Cs_2CuBr_4 is an exceptional material to study since it is very close to the maximum geometric frustration. By determining the specific-heat, the experimenters can also study effects from the gap in energies of low-lying magnetic excitation. The heat capacity of the sample is determined by applying heat to the sample and measuring the temperature difference the heat causes. This, however, depends largely on the temperature difference between the silver block of the calorimeter and the weak thermal links that are connected to the sapphire platform and the sample. Since it is possible that the thermal conductance of the weak links can change over time, it was the purpose of the experiment to design a program that would read the voltage of the platform and write the data to a file. This additional program will eliminate user error due to transcription of data and also allow future researchers to periodically verify the thermal conductance of the weak links. This in turn should allow for more accurate data analysis of the phase transitions for Cs_2CuBr_4 and other materials to be studied in the future.

Acknowledgments

I would like to thank Dr. Takano for the guidance and helpful discussions, as well as Younghak Kim for his assistance. This work was supported by the Center for Condensed Matter Sciences at the University of Florida Physics Department.

References

1. R. Moessner and A. P. Ramirez, Phys. Today **59**, 24 (2006).
2. A. P. Ramirez, J. Appl. Phys. **70**, 5952 (1991).

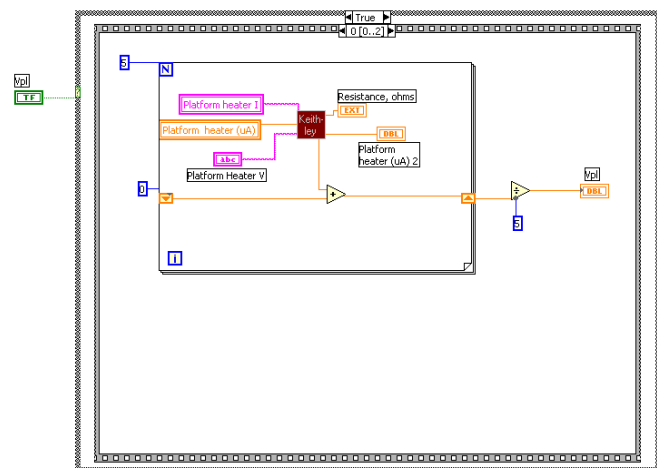


Figure 7: First sequence of True case

Figure 8 depicts the sequence used to write information to a second file. The “Decay start time” provides the first piece of information of each line with a time stamp. A tab is placed in between each additional piece of information. The file includes average temperature of the sample, the platform heater current, the platform voltage, the resistance of the block, the resistance of the platform when heater is off and the resistance of the platform when the heater is on. The voltage can be used in order to calculate the rate of heat flow. Thus, the thermal conductance of the weak links can be calculated by

$$k = \frac{\Delta Q}{\Delta t} * \frac{1}{A} * \frac{x}{\Delta T}$$

where k is the thermal conductance, $\frac{\Delta Q}{\Delta t}$ is the rate of heat flow, A is the surface are of the conducting surface, and $\frac{x}{\Delta T}$ is the inverse of the temperature gradient.

3. H. Tsujii *et al.*, Phys. Rev. B. **76**, 060406 (2007).

4. S. Nakatsuji *et al.*, Science **309**, 1697 (2005).

5. H. Kikuchi *et al.*, Phys. Rev. Lett. **94**, 227201 (2005).

6. R. Bachmann *et al.*, Rev. Sci. Instrum. **43**, 205 (1971).

7. H. Tsujii *et al.*, Physica B 329-333, 1638 (2003).